ASYMPTOTIC ANALYSIS OF THE UNDULAR HYDRAULIC JUMP OVER VANISHING BOTTOM SLOPE*

Murschenhofer D.† and Schneider W.
†Author for correspondence
Institute of Fluid Mechanics and Heat Transfer,
TU Wien,
Vienna,
Austria,
E-mail: dominik.murschenhofer@tuwien.ac.at

ABSTRACT

Stationary turbulent open-channel flow is considered for very large Reynolds numbers, and Froude numbers close to the critical value 1. In this double limit, the relative orders of magnitude are chosen such that the effect of vanishing bottom slope can be analyzed, independently from Reynolds and Froude numbers. By expanding the basic equations up to second order, an extended steady-state version of the Korteweg–de Vries (KdV) equation for the first-order perturbation of the surface elevation is obtained from a solvability condition, without the use of turbulence modeling or empirical constants. The investigation of numerical solutions of the extended KdV equation for vanishing slope shows a transition from an undular surface to the development of a single wave crest with breakdown afterwards within a very small range of slope reduction. A suitable choice of upstream boundary conditions for the extended KdV equation is suggested on the basis of an analysis of the transition to a fully developed state far downstream. The theory is compared with experimental data, and reasonable agreement is obtained.

INTRODUCTION

In hydraulics the transition from slightly supercritical to subcritical free-surface flow followed by a wave train with slowly decaying amplitude is known as the undular hydraulic jump, cf. [1, 2]. To investigate this phenomenon Grillhofer and Schneider [3] applied an asymptotic analysis to steady turbulent open-channel flow, considering a fully developed near-critical reference state far upstream. Provided the volume flow rate and the depth of the reference state are known for a given bottom slope, the analysis can be kept free of turbulence modeling. In a subsequent work Jurisits and Schneider [4] allowed for small deviations of the reference state from fully developed flow and derived an extended version of the Korteweg–de Vries (KdV) equation, describing the free-surface behaviour of near-critical flow in inclined channels with bottom slope α. In addition, a multiple-scaling method was applied to show that the extended KdV equation is uniformly valid, cf. [5]. Comparisons with experimental data as well as with numerical solutions of the Reynolds-averaged Navier–Stokes equations showed good agreement, [4–7].

For the special case of a horizontal bottom ($\alpha = 0$) one of the previous theory's basic assumptions, i.e. a *small* deviation from the fully developed flow, is violated. A straightforward modification of the theory for this case turned out to perform poorly in predicting the experimental data, [8]. Thus, the investigation of the limiting case of the bottom slope tending to zero appears promising to gain better understanding of the undular hydraulic

NOMENCLATURE

B	[-]	Coupling parameter
Fr	[-]	Froude number
Fr_τ	[-]	Friction Froude number
g	[m/s^2]	Acceleration due to gravity
h	[m]	Free surface elevation
m	[-]	Control parameter
p	[Pa]	Pressure
u	[m/s]	Velocity component in x-direction
u_τ	[m/s]	Friction velocity
v	[m/s]	Velocity component in y-direction
$\dot{V}$	[m^2/s]	Volume flow rate per unit width
x	[m]	Longitudinal coordinate
y	[m]	Lateral coordinate

Greek characters

α	[-]	Channel bottom slope
β	[-]	Dissipation parameter
γ	[-]	Parameter describing the deviation from a fully developed reference state
Γ	[-]	γ/β
δ	[-]	Contraction parameter for asymptotic expansion
ΔU	[-]	Non-dimensional velocity defect
$\Delta\overline{U'V'}$	[-]	Non-dimensional shear stress deviation from a fully developed reference state
ε	[-]	Perturbation parameter
ρ	[kg/m^3]	Density
τ_w	[Pa]	Wall shear stress

Subscripts

crit	Critical value
i	Initial value
r	Reference value
X	Partial derivative with respect to X
Y	Partial derivative with respect to Y
0	Leading order quantity
1	First-order perturbation quantity
2	Second-order perturbation quantity

*DEDICATED TO PROFESSOR KLAUS GERSTEN ON THE OCCASION OF HIS 90TH BIRTHDAY.

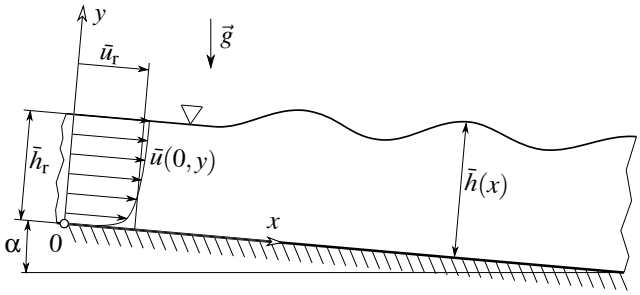

Figure 1. The stationary undular hydraulic jump in turbulent open-channel flow.

jump over horizontal bottoms and, furthermore, obtain sufficient agreement between analysis and experimental data.

GOVERNING EQUATIONS

Stationary turbulent open-channel flow over a plane bottom with slope $\alpha \to 0$ is considered, see Figure 1. The Reynolds number is assumed to be very large, and surface tension will be neglected. The Cartesian coordinate system is chosen such that the x axis is in the bottom plane, while the y axis points upwards. The corresponding velocity components are u and v, respectively. The time-averaged flow is assumed to be two-dimensional with given volume flow rate per unit width of the channel, $\dot{V}$. Time-averaged quantities are denoted by a bar and fluctuations around the average by a prime. The time-averaged surface elevation is $\bar{h}(x)$. The origin of the coordinate system is at a position upstream of the undular jump, where the flow is slightly supercritical. This upstream state is chosen as reference state (subscript r), with surface height $\bar{h}_r = \bar{h}(0)$ and volumetric mean velocity $\bar{u}_r = \dot{V}/\bar{h}_r$ serving as a reference length and a reference velocity, respectively. The pressure p is referred to the hydrostatic pressure $\rho g \bar{h}_r$ at the bottom of the channel in the reference state, where ρ is the constant fluid density and g is the acceleration due to gravity. The Reynolds stresses are referred to the square of the reference friction velocity, $u_{\tau,r}^2$, where $u_\tau = \sqrt{\tau_w/\rho}$ with the wall shear stress τ_w at the bottom of the channel.

The following governing equations and boundary conditions have been adopted unchanged from the previous analysis by Jurisits and Schneider [4]. Thus, non-dimensional variables are introduced as follows:

$$\begin{aligned} &X = \delta\, x/\bar{h}_r\,, \qquad Y = y/\bar{h}_r\,, \qquad \bar{H} = \bar{h}/\bar{h}_r\,, \qquad \bar{U} = \bar{u}/\bar{u}_r\,, \\ &\bar{V} = \delta^{-1}\bar{v}/\bar{u}_r\,, \qquad \bar{P} = \bar{p}/(\rho g \bar{h}_r)\,, \qquad U_\tau = u_\tau/u_{\tau,r}\,, \\ &\overline{U'^2} = \overline{u'^2}/u_{\tau,r}^2\,, \qquad \overline{V'^2} = \overline{v'^2}/u_{\tau,r}^2\,, \qquad \overline{U'V'} = \overline{u'v'}/u_{\tau,r}^2\,, \end{aligned} \tag{1}$$

with the small parameter δ introduced to contract the longitudinal coordinate in the asymptotic expansion, see below.

The continuity equation for incompressible flow in non-dimensional form reads

$$\bar{U}_X + \bar{V}_Y = 0\,, \tag{2}$$

where the subscripts X and Y denote partial derivatives with respect to X and Y, respectively.

For very large Reynolds numbers the flow field can be divided into a viscous wall layer adjacent to the channel bottom and a non-viscous defect layer that forms the bulk of the flow field [9]. As the viscous wall layer is known to have universal properties, cf. also [9], it suffices to consider only the defect layer in what follows. Then the equations of motion are

$$\delta \mathrm{Fr}^2(\bar{U}\bar{U}_X + \bar{V}\bar{U}_Y) = -\delta\bar{P}_X + \alpha - \mathrm{Fr}_\tau^2(\delta\,\overline{U'^2}_X + \overline{U'V'}_Y)\,, \tag{3a}$$

$$\delta^2 \mathrm{Fr}^2(\bar{U}\bar{V}_X + \bar{V}\bar{V}_Y) = -\bar{P}_Y - 1 - \mathrm{Fr}_\tau^2(\delta\,\overline{U'V'}_X + \overline{V'^2}_Y)\,, \tag{3b}$$

where the Froude numbers are defined as

$$\mathrm{Fr} = \frac{\bar{u}_r}{\sqrt{g\bar{h}_r}}\,, \qquad \mathrm{Fr}_\tau = \frac{u_{\tau,r}}{\sqrt{g\bar{h}_r}}\,. \tag{4}$$

For large Reynolds numbers the effects of friction are known to be small. Hence, it can be assumed that the friction Froude number is very small, that is, $\mathrm{Fr}_\tau \ll 1$, while Fr is slightly above the critical value 1.

The system of basic equations (2), (3a) and (3b) is to be solved subject to appropriate boundary conditions. At the bottom, the conventional boundary condition for the lateral velocity, i.e. $\bar{V}(X,0) = 0$, is prescribed. Matching with the viscous wall layer yields the boundary condition for $\overline{U'V'}$ at the bottom, cf. [4] equation (9), and a coupling condition for U_τ and $\bar{H}$, cf. [4] equations (6-8). At the free surface conventional kinematic and dynamic boundary conditions are imposed, meaning, the averaged interface is defined by a streamline in the averaged velocity field, i.e.

$$\bar{V}(X,\bar{H}) = \bar{U}(X,\bar{H})\,\bar{H}_X\,, \tag{5}$$

and continuity of stresses is expressed by the relations

$$\left[\bar{P}(X,\bar{H}) + \mathrm{Fr}_\tau^2\,\overline{U'^2}(X,\bar{H})\right]\delta\bar{H}_X - \mathrm{Fr}_\tau^2\,\overline{U'V'}(X,\bar{H}) = 0\,, \tag{6a}$$

$$\left[\bar{P}(X,\bar{H}) + \mathrm{Fr}_\tau^2\,\overline{V'^2}(X,\bar{H})\right] - \mathrm{Fr}_\tau^2\,\overline{U'V'}(X,\bar{H})\,\delta\bar{H}_X = 0\,. \tag{6b}$$

ASYMPTOTIC ANALYSIS

The undular hydraulic jump is known to appear only if the upstream Froude number, Fr, is slightly above the critical value 1, cf. [1, 2, 10]. It is also known that the wave lengths in an undular jump are large in comparison to the water depth. Thus, following [3–5], a small perturbation parameter ε is introduced according to

$$\mathrm{Fr} = 1 + \frac{3}{2}\varepsilon\,, \qquad \varepsilon \to 0\,, \tag{7}$$

and the contraction parameter is defined as

$$\delta = 3\sqrt{\varepsilon}, \tag{8}$$

where the coefficients $3/2$ and 3 serve for simplifying the final result.

Guided by relationships that apply to fully developed flow, it was assumed in previous works [3–5] that the bottom slope as well as the friction Froude number vanish with vanishing ε. Obviously, that approach is not suitable for studying undular jumps in the limit of vanishing bottom slopes. Thus, the basic idea of the present work is to introduce a coupling between the non-dimensional parameters that satisfies the following two requirements: First, the limit $\alpha \to 0$ ought to be carried out with ε and Fr_τ fixed, at least in the first order. Second, allowing to perform the analysis without the use of any turbulence modeling or empirical parameters. These requirements can be satisfied by coupling the parameters as follows:

$$\begin{aligned} &\alpha = \mathrm{Fr}_\tau^2(1-\varepsilon^{3m}) = 3\mathrm{Fr}_\tau^2\, m\ln(1/\varepsilon) + \ldots \\ &\text{with} \quad m\ln(1/\varepsilon) \to 0\,; \qquad \mathrm{Fr}_\tau^2 = B\,\varepsilon^{5/2-m}, \end{aligned} \tag{9}$$

where the coupling parameter is a constant of the order 1, i.e., $B = \mathrm{O}(1)$. Thus, the vanishing bottom slope is controlled by the exponent m.

The dependent variables are now expanded in terms of powers of ε, e.g.,

$$\begin{aligned} \bar{H}(X) &= H_0 + \varepsilon H_1(X) + \varepsilon^2 H_2(X) + \mathrm{O}(\varepsilon^3)\,, \\ \bar{U}(X,Y) &= U_0 + \varepsilon U_1(X,Y) + \varepsilon^2 U_2(X,Y) + \mathrm{O}(\varepsilon^3)\,, \\ \bar{P}(X,Y) &= P_0(Y) + \varepsilon P_1(X,Y) + \varepsilon^2 P_2(X,Y) + \mathrm{O}(\varepsilon^3)\,, \end{aligned} \tag{10}$$

neglecting terms of order ε^3 and smaller.

Expanding the governing equations and boundary conditions accordingly, the leading order terms represent the basic state:

$$U_0 = 1, \qquad V_0 = 0, \qquad P_0 = 1 - Y, \qquad H_0 = 1. \tag{11}$$

The leading order of the Reynolds shear stresses is assumed to be of the form

$$(\overline{U'V'})_0 = Y - 1 + \Delta\overline{U'V'}(Y)\,, \tag{12}$$

where the term $\Delta\overline{U'V'}(Y)$ allows for a deviation in the reference state from the linear profile of the fully developed flow. Of course, the term $\Delta\overline{U'V'}(Y)$ has to comply with the boundary conditions at the bottom and the free surface, respectively, i.e. $\Delta\overline{U'V'}(0) = \Delta\overline{U'V'}(1) = 0$. Note that $(\overline{U'V'})_0$ does not appear in the leading order of the equation of motion, (3a), since the term is multiplied with Fr_τ^2, and thus shifted to a higher order.

In the next step, the following relationships are obtained for the first-order perturbation quantities:

$$U_1 = -H_1 + \sqrt{B}\,\varepsilon^{(1-2m)/4}\Delta U(Y)\,, \quad V_1 = H_{1X}Y, \quad P_1 = H_1. \tag{13}$$

The term $\Delta U(Y)$ represents the velocity defect in the reference state. With flows close to separation being excluded, the velocity defect is of the order of the friction velocity [9], i.e. $\bar{U}(0,Y) = 1 + \mathrm{Fr}_\tau\,\Delta U(Y)$ with $\Delta U(Y) = \mathrm{O}(1)$. Since a volumetric mean value has been chosen as reference velocity, the integral of $\Delta U(Y)$ over the whole channel cross section vanishes per definitionem. As a consequence, $\Delta U(Y)$ will not appear in the final result of the analysis.

Without turbulence modeling, the first-order perturbation of the Reynolds shear stresses can be determined only at the boundaries, i.e.

$$(\overline{U'V'})_1(X,0) = 2H_1\,, \quad (\overline{U'V'})_1(X,1) = -H_1 - (\Delta\overline{U'V'})_Y(1)\,. \tag{14}$$

The first equation in (14) is obtained by expanding the logarithmic law up to first-order terms, using the relation $-\overline{U'V'} = U_\tau$ as $Y \to 0$, cf. [4] equations (6-9). The second equation follows from the dynamic boundary condition at the free surface, (6a), neglecting terms of order ε^{1+m} and smaller.

$H_1(X)$ remains free in the framework of the first-order equations and is to be determined from a solvability condition of the second-order equations. Performing the analysis as described in [3, 4] the second-order perturbation equations resulting from the momentum equation in X-direction, (3a), and from the kinematic boundary condition, (5), respectively, are compatible if

$$H_{1XXX} + H_{1X}(H_1 - 1) = \beta\left[H_1 + \frac{1}{3}(\Delta\overline{U'V'})_Y(1)\right] - \gamma, \tag{15}$$

with

$$\beta = \frac{B}{3}\varepsilon^{1-m} = \frac{\mathrm{Fr}_\tau^2}{3\varepsilon^{3/2}}\,, \qquad \gamma = \frac{B}{9}\varepsilon^{2m} = \frac{\mathrm{Fr}_\tau^2 - \alpha}{9\varepsilon^{5/2}}\,. \tag{16}$$

In order to avoid turbulence modeling it is assumed that

$$(\Delta\overline{U'V'})_Y(1) \ll 1\,. \tag{17}$$

An a posteriory justification of this assumption will be provided in the last paragraph of this section.

If (17) is satisfied, (15) simplifies to the non-linear third-order ordinary differential equation

$$H_{1XXX} + H_{1X}(H_1 - 1) = \beta H_1 - \gamma, \tag{18}$$

describing, in a first approximation, the surface elevation as a function of the contracted longitudinal coordinate X. Equation (18) is known [4] as a steady-state version of the KdV equation extended by a linear dissipation term (βH_1) and a constant γ that represents the deviation of the reference state from fully developed flow.

Dropping the term H_{1XXX} in (18) leads to the one-dimensional flow approximation (or "hydraulic approximation") in the limit $\varepsilon \to 0$ [11][1]. Obviously, with the term H_{1XXX} missing, equation (18) becomes singular as the surface elevation approaches the critical value $H_1 = 1$. This shows the inability of the one-dimensional flow approximation of classical hydraulics to describe undular jumps. However, it may serve as an approximate solution for the flow upstream of the undular jump. An example will be given below. For that purpose (18) is integrated after dropping the term H_{1XXX}, choosing $H_1(0) = 0$ as boundary condition, to obtain the following implicit solution for $H_1(X)$ in one-dimensional ("hydraulic") approximation:

$$X(H_1) = [H_1 + (\Gamma - 1)\,\ln(1 - H_1/\Gamma)]/\beta\,, \qquad (19)$$

with $\Gamma = \gamma/\beta$. We shall see that (19) can be also used to determine appropriate initial conditions for (18), i.e. initial value $H_1(X_\mathrm{i})$, slope $H_{1X}(X_\mathrm{i})$ and curvature $H_{1XX}(X_\mathrm{i})$, for any value $X = X_\mathrm{i}$ chosen sufficiently far away from the critical value $X = X_\mathrm{crit}$, where $H_1 = 1$.

If the term H_{1XXX} were dropped in (15) rather than (18), the result would not be in accord with the hydraulic approximation. Thus, the assumption (17) is consistent with describing the flow upstream of the hydraulic jump with the equations of the hydraulic theory.

RESULTS AND DISCUSSION

Equation (18) can be solved numerically with standard methods using the the commercial software Matlab R2017a. Solutions of the initial value problem are obtained with the function ode45 and a relative error tolerance of 10^{-4}, an absolute error tolerance of 10^{-6} and a maximum step size of 10^{-4}. The two-point boundary-value problem is solved by means of the function bvp4c. To satisfy the residuum of 10^{-5}, about 1900 points on an interval $X \in [-18.46,\ 100]$ were used.

Numerical solutions of the extended KdV equation for $\alpha \to 0$

As mentioned above it is the purpose of this work to investigate the behavior of the undular hydraulic jump as the bottom slope $\alpha \to 0$ independently from ε and Fr_τ. In Figure 2 solutions of the extended KdV equation (18) are shown for fixed values $\mathrm{Fr} = 1.06$ and $\mathrm{Fr}_\tau = 0.015$. The critical bottom slope, i.e., the slope at which the reference state would be fully developed, is $\alpha_\mathrm{crit} = \mathrm{Fr}_\tau^2 = 2.25 \cdot 10^{-4}$. Choosing α smaller than the critical slope, e.g. $\alpha = 1.84 \cdot 10^{-4}$ (black curve), yields a solution that leads to a pool of liquid with horizontal surface far downstream

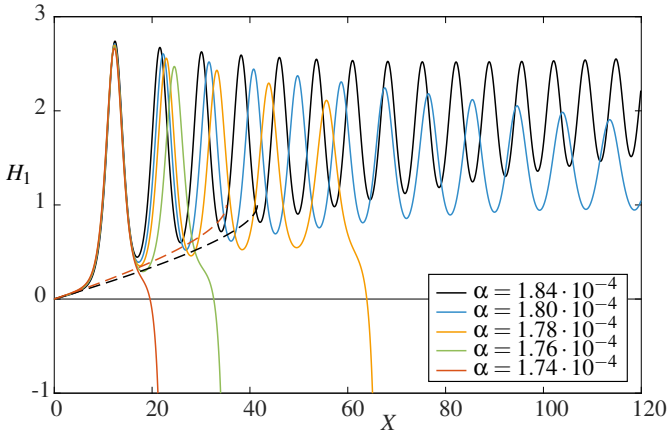

Figure 2. Numerical solutions of (18) for very small bottom slopes. $\mathrm{Fr} = 1.06$, $\mathrm{Fr}_\tau = 0.015$; $\beta = 9.38 \cdot 10^{-3}$, γ according to (16) ranging from $\gamma = 1.42 \cdot 10^{-2}$ ($\alpha = 1.84 \cdot 10^{-4}$) to $\gamma = 1.77 \cdot 10^{-2}$ ($\alpha = 1.74 \cdot 10^{-4}$). Initial conditions $H_1(0) = 0$, $H_{1X}(0) = \gamma$ and $H_{1XX}(0) = \gamma^2$. Dashed lines represent solutions of (19) for $\alpha = 1.84 \cdot 10^{-4}$ (black) and $\alpha = 1.74 \cdot 10^{-4}$ (red).

('deep water'), cf. [4]. Slightly reducing the α value (blue, orange and green curves) leads to solutions with a breakdown at some distance downstream. With decreasing slope also the number of wave crests decreases until a single crest with breakdown immediately afterwards remains for $\alpha = 1.74 \cdot 10^{-4}$ (red curve). For a horizontal bottom a breakdown of the solution is not surprising since a fully developed state does not exist. However, it is remarkable that by reducing the slope by 10^{-5}, which is far beyond the usual measurement uncertainty in experiments, the solution of (18) undergoes a transition from approaching 'deep water' far downstream to only one wave crest with still almost the same amplitude. Note that for varying α, according to (16) only the parameter γ changes, i.e. $\gamma \to \mathrm{O}(1)$ as $\alpha \to 0$. Thus, the damping effect of γ becomes dominant and undulations are suppressed.

The black and red dashed curves in Figure 2 represent solutions of (19) for $\alpha = 1.84 \cdot 10^{-4}$ and $\alpha = 1.74 \cdot 10^{-4}$, respectively. This shows that the critical value X_crit decreases with decreasing slope. More precisely, $X_\mathrm{crit} \to [1 + (1/(3\varepsilon) - 1)\,\ln(1 - 3\varepsilon)]/\beta$ as $\alpha \to 0$, that is, $X_\mathrm{crit} \to 6.67$ for the chosen values of ε and Fr_τ. As will be discussed later, it is reasonable to choose an initial point X_i for the solution of (18) at the corresponding solution of (19). For the sake of comparison in Figure 2 the common initial point for all solid curves is $X_\mathrm{i} = 0$, which is the only point where all curves according to (19) intersect.

Transition to fully developed flow far downstream

However small but different from 0 the bottom slope might be a fully developed state far downstream exists provided $\Gamma > 1$. Thus, the current analysis of vanishing bottom slope includes this special case, which is characterized by the downstream boundary condition $H_1 = \Gamma$ as $X \to \infty$, cf. [4, 11].

In Figure 3 the numerical solution of (18) as a two-point boundary-value problem with $\beta = 0.12$ and $\Gamma = 1.8$ is shown as

[1] Due to an unusual definition of the local friction coefficient, the equation given in [11] differs from the present one by a coefficient 5/3 in the β-term.

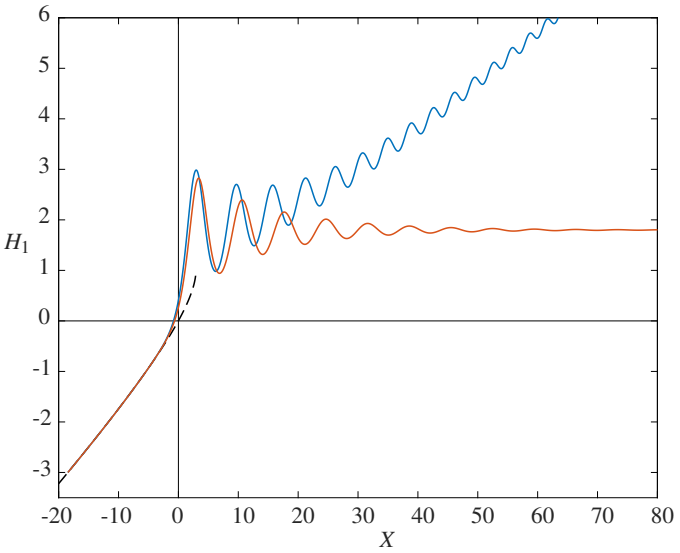

Figure 3. Numerical solutions of (18) with $\beta = 0.12$, $\Gamma = 1.8$. Red line: two-point boundary-value problem; $H_1(-18.46) = -3$, $H_{1X}(-18.46) = 0.144$, $H_1(100) = 1.8$. Blue line: initial value problem; $H_1(-18.46) = -3$, $H_{1X}(-18.46) = 0.144$, $H_{1XX}(-18.46) = 9.01 \cdot 10^{-2}$. Dashed line: solution of (19).

a red curve. The boundary conditions at the upstream boundary are obtained by determining the position X_i and the corresponding slope $H_{1X}(X_i)$ from (19) for the chosen value $H_1(X_i) = -3$. It is assumed that $X = 100$ is sufficiently far downstream to prescribe the asymptotic boundary condition, i.e. $H_1(100) = \Gamma = 1.8$. Interestingly, the solution of (18) closely follows the one-dimensional approximation (dashed line) for quite a large distance. Nevertheless, shortly before the origin of the coordinate system, the solution of (18) develops into an undular jump with strongly decaying amplitude. This behavior indicates that the extended KdV equation (18) is not only uniformly valid downstream of the jump, [5], but also is able to accurately represent the inflow.

The curvature of the red curve at the initial point $X_i = -18.46$ is 4.24% larger than the curvature of the solution of the corresponding hydraulic approximation, (19), at this position. Using the enlarged curvature, together with the initial value and initial slope prescribed for the two-point boundary-value problem, to solve (18) as an initial value problem yields the blue curve in Figure 3. As discussed in [11] the numerical error always gives rise to a solution of the initial value problem approaching the asymptote $H_1 = \beta X$ rather than $H_1 = \Gamma$ as $X \to \infty$. However, initially also the blue curve closely follows the solution of the hydraulic theory, (19). It appears that choosing $X_i = 0$ as the upstream boundary for the two-point boundary-value problem as well as for the initial value problem, as it was done in previous works [4, 11], has to be taken with reservations, since the solutions of (18) bifurcate from the one-dimensional hydraulic theory already before, see Figure 3.

Comparison with experimental data

Only very few experiments of the undular hydraulic jump over *horizontal* bottom with detailed measurement of the surface elevation are available in the literature. Reinauer and Hager [12] conducted their experiment at $\mathrm{Fr} = 1.36$, which reportedly represents the limiting case to wave breaking. Gotoh et al. [13] presented a horizontal experiment with $\mathrm{Fr} = 1.5$. Both experiments will not be used for comparison, since the Froude numbers are relatively large and the similarity parameter B, representing a measure for the validity of the present theory, is smaller than the corresponding perturbation parameter ε. The experiment by Chanson [14], CD1, with $\mathrm{Fr} = 1.266$ and $\mathrm{Fr}_\tau = 5.54 \cdot 10^{-2}$ (i.e. $\varepsilon = 0.177$, $B = 0.23$) seems to be the most suitable for comparison with the present theory, even though the experimental configuration leads to a value of B which is rather of order ε than of order 1, and, furthermore, a recirculation bubble below the first wave crest was observed, whereas flow reversal is excluded in the present analysis. Since the analysis is based on the assumption of vanishing, but nonzero bottom slope, a very small but finite value $\alpha = 10^{-8}$ is chosen for the following comparison.

In Figure 4 the measured surface elevation [14] is represented by squares. Chanson [14] indicates an uncertainty in the measurement of the volume flow rate $\dot{V}$ of about 2%. Therefore, solutions of (18) were first obtained for a parameter set corresponding to $\dot{V} = 0.0914\ \mathrm{m}^2/\mathrm{s}$ as reported by Chanson [14] (blue solid curve) and then for parameters corresponding to a 2% smaller volume flow rate (red solid curve). Both the blue and red solid curve is shifted along the corresponding solution of (19), i.e. the blue and red dashed line, respectively, such that the first wave

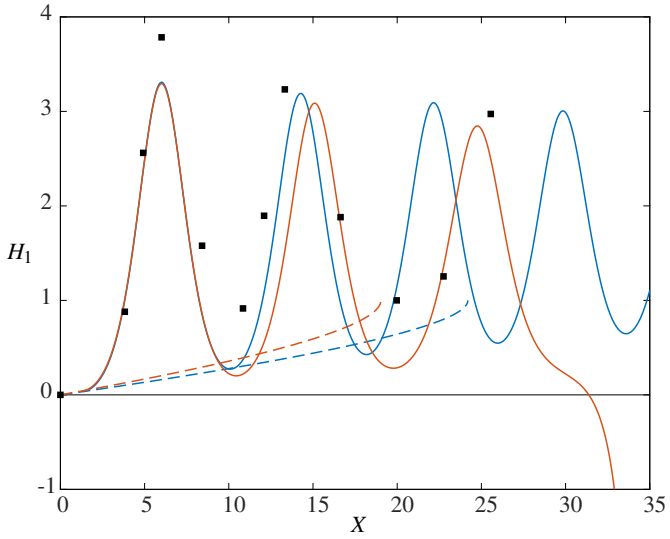

Figure 4. Comparison of the surface observed by Chanson [14] (squares) with numerical solutions of (18) (solid lines), for initial conditions: $H_1(0) = 0$, $H_{1X}(0) = \gamma$, $H_{1XX}(0) = 0.2$. Blue curves: $\varepsilon = 0.177$, $\beta = 1.37 \cdot 10^{-2}$, $\gamma = 2.58 \cdot 10^{-2}$; red curves: $\varepsilon = 0.16$, $\beta = 1.53 \cdot 10^{-2}$, $\gamma = 3.19 \cdot 10^{-2}$. Dashed lines: solutions of (19). Experimental data: $\mathrm{Fr} = 1.266$, $\bar{h}_r = 81$ mm, $\dot{V} = 0.0914\ \mathrm{m}^2/\mathrm{s}$.

crest is in accord with the experimental data. Whereas the first wave crest of both solid curves is of almost the same shape, the successive crests show significant differences, especially with respect to the wave length. Reasonable agreement between experimental data and the solution of the extended KdV equation (18) is obtained only by incorporating the measurement uncertainty. This indicates the sensitivity of the surface elevation with respect to small changes in the volume flow rate, as already observed in [3, 11].

CONCLUSIONS

The problem of the undular hydraulic jump over a plane bottom with a slope approaching zero was investigated by an asymptotic expansion for large Reynolds numbers, and Froude numbers close to the critical value 1. It was possible to keep the first-order results free of turbulence modeling by restricting the investigation to a certain parameter regime that is characterized by a coupling parameter being of order 1 and a constraint for the deviation of the Reynolds shear stresses from the linear profile of fully developed flow in the reference state. With Reynolds and Froude numbers fixed, the vanishing bottom slope was shown to be controlled by an additional parameter, as defined in (9). The main result of the analysis is equation (18), that is, an already known extended steady-state version of the KdV equation for the surface elevation.

Numerical solutions of (18) as an initial value problem were analyzed by solely altering the bottom slope α. As α decreases, the number of undulations decreases until eventually one single wave crest with immediate breakdown afterwards remains.

The comparison of theoretical results with the most suitable experiment found in the literature, i.e. [14], turned out to be rather sensitive to relatively small uncertainties in the data. However, in view of the remarkable fact that the analytical results are free of empirical constants, the agreement between theory and experiment can be considered satisfactory.

A comparison of solutions of (18) as an initial value problem and as a two-point boundary-value problem, respectively, was performed, choosing a common initial point upstream of the jump. The results suggest that in both cases proper upstream boundary conditions should be chosen sufficiently far upstream of the jump and in accord with the one-dimensional flow approximation, i.e., (19). Moreover, it is shown that numerical errors give rise to a solution of the initial value problem approaching a pool of liquid with horizontal surface rather than the fully developed flow far downstream, as prescribed in the two-point boundary-value problem; cf. [11] for a more detailed discussion.

Concerning future work, the effect of vanishing bottom slope on the solution of (18) as a two-point boundary-value problem will be analyzed in [15]. Preliminary results indicate that, in contrast to the initial value problem, the damping decreases with decreasing α, resulting in an increasing number of wave crests.

ACKNOWLEDGMENT

Financial support by Androsch International Management Consulting GmbH (AIC) is gratefully acknowledged.

REFERENCES

[1] Chow V.T., Open-Channel Hydraulics, McGraw-Hill, New York, 1959.

[2] Castro-Orgaz O. and Hager W.H., Non-Hydrostatic Free Surface Flows, Springer, 2017.

[3] Grillhofer W. and Schneider W., The undular hydraulic jump in turbulent open channel flow at large Reynolds numbers, *Physics of Fluids*, Vol. 15, 2003, pp. 730–735.

[4] Jurisits R. and Schneider W., Undular hydraulic jumps arising in non-developed turbulent flows, *Acta Mechanica*, Vol. 223, 2012, pp. 1723–1738.

[5] Steinrück H., Multiple scales analysis of the turbulent undular hydraulic jump, In: Asymptotic Methods in Fluid Mechanics: Survey and Recent Advances, Edited by H. Steinrück, CISM Courses and Lectures, No. 523, Springer, Wien New York, 2010, pp. 197–219.

[6] Jurisits R., Schneider W. and Bae Y.S., A multiple-scales solution of the undular hydraulic jump problem, *Proceedings in Applied Mathematics and Mechanics*, Vol. 7, 2007, pp. 4120007–4120008.

[7] Schneider W., Jurisits R. and Bae Y.S., An asymptotic iteration method for the numerical analysis of near-critical free-surface flows, *International Journal of Heat and Fluid Flow*, Vol. 31, 2010, pp. 1119–1124.

[8] Murschenhofer D. and Schneider W., Multiple scales analysis of the undular hydraulic jump over horizontal surfaces, *Proceedings in Applied Mathematics and Mechanics*, 2019, to be submitted.

[9] Schlichting H. and Gersten K., Boundary-Layer Theory, 9th Ed., Springer, Berlin Heidelberg, 2017.

[10] Chanson H. and Montes J.S., Characteristics of Undular Jumps: Experimental Apparatus and Flow Patterns, *Journal of Hydraulic Engineering*, Vol. 121, 1995, pp. 129–144.

[11] Jurisits R., Wellige Wassersprünge bei nicht voll ausgebildeter turbulenter Zuströmung, Dissertation, TU Wien, Vienna, 2012.

[12] Reinauer R. and Hager W., Non-breaking undular hydraulic jump, *Journal of Hydraulic Research*, Vol. 33, 1995, pp. 683–698.

[13] Gotoh H., Yasuda Y. and Ohtsu I., Effect of channel slope on characteristics of undular hydraulic jump, In: River Basin Management III, Edited by C.A. Brebbia and J.S.A. do Carmo, WIT Transactions on Ecology and the Environment, Vol. 83, WIT Press, Southampton, 2005, pp. 33–43.

[14] Chanson H., Physical modelling of the flow field in an undular tidal bore, *Journal of Hydraulic Research*, Vol. 43, 2005, pp. 234–244.

[15] Murschenhofer D., Near-critical turbulent free-surface flows over horizontal and nearly horizontal bottoms, Dissertation, TU Wien, Vienna, in preparation.